PHYSICAL REVIEW D VOLUME 29, NUMBER 5 1 MARCH 1984

Glueball-mass estimates in lattice QCD

Herbert W. Hamber and Urs M. Heller
The Institute for Advanced Study, Princeton, New Jersey 08540
(Received 21 March 1983)

We show how the Langevin equation for SU(3) gauge fields can be used to compute glueball correlation functions at large separation. On a $6\times6\times6\times6$ lattice we estimate the mass of the lowest 0^{++} glueball by determining the corresponding correlation function at separations 0, 1, 2, and 3. Several values for the coupling constant are investigated which lie in a region where scaling behavior for the string tension is observed. Our preliminary study indicates $m_{0^{++}}=(240\pm70)\Lambda_0$ or alternatively $m_{0^{++}}=(1.1\pm0.2)m_\rho$.

I. INTRODUCTION

The lattice gauge theory presents a well defined framework in which nonperturbative effects in QCD can be studied. One of the more fruitful techniques in this respect has been the Monte Carlo method. Several attempts have been made to extract the mass of the lightest state, the scalar glueball, in the pure gauge theory.[1-8] An appropriate connected two-point correlation function of operators that have the quantum numbers of the glueball is evaluated numerically, and from its large-distance exponential falloff the mass of the lowest state is extracted.

In the currently studied coupling-constant regime the lowest masses are of order one in lattice units, which implies that the correlation functions themselves become rapidly very small as the separation is increased. The statistical fluctuations in a numerical simulation are of order $N^{-1/2}$, where N is the number of Monte Carlo sweeps per variable over which the averaging is done. Because of this signal-to-noise-ratio problem one is limited in practice to rather short distances over which the correlation functions can be evaluated, if machine time is to be kept within reasonable limits. Also, as the gauge coupling becomes weaker it is necessary to determine the correlation functions at larger distances in order to separate the exponential tail from the uninteresting short-distance power behavior.

Glueball-mass estimates have been limited in the past to a study of correlations at distances 1 and 2, and in some rare instances 3.[2-7] An exception is Ref. 8 in which for the group SU(2) the glueball correlation function was determined up to separation 5. On the other hand, there is in general no reason to believe that the true asymptotic behavior of the correlation function is reached at such short distances. In Ref. 9 it was suggested that the Langevin equation could be used for computing connected glueball correlation functions, with an increase in accuracy of several orders of magnitude over the Monte Carlo method, and some calculations were performed for the group SU(2). The increase in accuracy is achieved by allowing for a coherent cancellation of statistical errors between two highly correlated stochastic processes.

In this paper the analysis is extended to the group SU(3). After introducing the Langevin equation for the group SU(3), we calculate the connected glueball correlation function at $\beta=5.4$, 5.5, 5.6, 5.7, and 5.8 and extrapolate the results for the glueball mass to the continuum limit using the renormalization group. Our results are in reasonable agreement with previous results (for a list of references to previous work we refer the reader to refs. 2 and 4, though they tend to indicate slightly lower values for the mass of the lowest 0^{++} glueball state.

The plan of the paper is as follows. In Sec. II we introduce the Langevin equation on the group manifold of SU(3) and discuss its time-discretized form. Then it is shown how the connected two-point correlation function can be evaluated by setting up two closely correlated processes with slightly different parameters in the actions. Section III goes into the details of the numerical simulation and presents our results, together with a discussion of statistical and systematic errors. In Sec. IV we discuss our results and compare to previous similar calculations. After pointing out the importance of extraneous effects such as the presence of a peak in the specific heat in the region where the masses are calculated and the spin-wave behavior of the correlation function at short distances, we discuss the extrapolation of the masses to the continuum limit.

II. THE LANGEVIN EQUATION FOR SU(3)

Let us first establish some notation. The gauge degrees of freedom are defined on the links of a four-dimensional periodic hypercubic lattice of spacing a and linear size L, and are elements of the group SU(3). We use the Wilson form of the action[10]

$$S_G=-\frac{\beta}{6}\sum_{n,\mu<\nu}\mathrm{Tr}U_{n,\mu}U_{n+\mu,\nu}U^{\dagger}_{n+\nu,\mu}U^{\dagger}_{n,\nu}+\text{c.c.} \quad (2.1)$$

with $\beta=6/g^2$.

It is known that the Langevin equation[9] represents a useful alternative to the Monte Carlo method for generating a set of equilibrium configurations.[11-13] Given a field $\varphi(x)$ in the continuum, one introduces an extra time t and writes down the evolution equation

$$\dot{\varphi}(x,t)=-\frac{\delta S}{\delta\varphi}+\eta(x,t)\ , \tag{2.2}$$

where $\eta(x,t)$ is a Gaussian white noise

$$\begin{aligned}&\langle\eta(x,t)\rangle=0\ ,\\&\langle\eta(x,t)\eta(x',t')\rangle=2\delta(x-x')\delta(t-t')\ .\end{aligned} \tag{2.3}$$

In order to solve the above equation numerically, one needs to discretize the time. With a time step ϵ and $t=\epsilon k$, Eq. (2.3) becomes

$$\varphi^{(k+1)}(x)=\varphi^{(k)}(x)-\epsilon\frac{\delta S}{\delta\varphi}\bigg|_{\varphi=\varphi^{(k)}}+(2\epsilon)^{1/2}\eta^{(k)}(x) \tag{2.4}$$

with

$$\begin{aligned}&\langle\eta^{(k)}(x)\rangle=0\ ,\\&\langle\eta^{(k)}(x)\eta^{(k')}(x')\rangle=\delta(x-x')\delta_{kk'}\ .\end{aligned} \tag{2.5}$$

This procedure introduces an error of order ϵ in the averages, which can in principle be reduced by going to small enough ϵ. It is possible to write down equations such that the detailed balance condition for the transition probabilities $P(c,c')$

$$e^{-S(c)}P(c,c')=P(c',c)e^{-S(c')} \tag{2.6}$$

is enforced to higher order in ϵ. Algorithms exist for which the error is of order ϵ^2, but they are rather complicated.[14]

The Langevin equation for Dirac fermions is also known and is discussed in Refs. 15 and 16 in the context of lattice gauge theories. Here we are interested in writing evolution equations for elements of the group SU(3). It is easy to show that the correct equilibrium distribution is recovered, up to order ϵ, if the matrices $U_{n\mu}$ evolve according to the stochastic equation[17,18]

$$U_{n\mu}^{(k+1)}=\exp\left\{i(2\epsilon)^{1/2}\omega_{n\mu}^{\alpha}\frac{\lambda_\alpha}{2}-\epsilon P_{AT}\left[\frac{\delta S}{\delta U_{n\mu}^{(k)}}U_{n\mu}^{(k)}\right]\right\}U_{n\mu}^{(k)}\ . \tag{2.7}$$

Here the λ_α's are the Gell-Mann matrices, generators of the group SU(3), and the $\omega_{n\mu}^{\alpha}$'s are random real numbers with zero mean and unit variance

$$\begin{aligned}&\langle\omega_{n\mu}^{\alpha}\rangle=0\ ,\\&\langle\omega_{n\mu}^{\alpha}\omega_{n'\mu'}^{\beta}\rangle=\delta_{nn'}\delta_{\mu\mu'}\delta^{\alpha\beta}\ .\end{aligned} \tag{2.8}$$

The operator P_{AT} projects out the anti-Hermitian traceless part of the operator in parentheses. Its effect is to constrain the new element to lie still on the group manifold. The force term $\delta S/\delta U_{n\mu}$ contains the effect of the $6(d-1)$ neighboring links, and, in the case when fermion degrees of freedom are present, will include the contribution from the fermion currents.

In practice we prefer not to take the exponential of an operator, such as written in Eq. (2.7). The random SU(3) matrices

$$R_{n\mu}(\epsilon)=\exp\left[i(2\epsilon)^{1/2}\omega_{n\mu}^{\alpha}\frac{\lambda_\alpha}{2}\right] \tag{2.9}$$

are computed by expanding the exponential to fourth order (which is justified for small ϵ) and projecting them uniformly on the group. This is achieved, for example, by choosing at random a row or column of R, and orthonormalizing the remaining rows (viz., columns) with respect to the chosen one.[19] We have checked that the error introduced by this procedure is negligible (we typically use ϵ of order 10^{-3}). A table of 200 random R matrices (containing always both R and R^+ to ensure detailed balance) is updated every time a full sweep through the lattice is completed.

Because of the smallness of ϵ we have also chosen to expand the force contribution in Eq. (2.7) to lowest order in ϵ. The deviations from unitarity of the new matrices $U_{n\mu}^{(k+1)}$, which arises because we neglect higher-order contributions in ϵ, are corrected by projecting the matrices back on the group in the same way as described above for the $R_{n\mu}$ matrices.

In order to speed up the approach toward thermal equilibrium each link matrix $U_{n\mu}$ is updated ten times before we proceed to the next link. As we will show in the next section, we have checked that our procedure reproduces the correct energy density (average plaquette) with an error of order ϵ.

Let us now discuss the determination of the correlation functions.[9] In order to compute the connected correlation function of two glueball operators, we set up two correlated stochastic processes. We consider two initially identical systems E_0 and E_1, which are in thermal equilibrium at a temperature β. E_0 is then allowed to further evolve in time according to the evolution equations (2.7). In system E_1 the action is changed to

$$S\rightarrow S-\delta\tilde{O}(t_0)\ , \tag{2.10}$$

where the operator $\tilde{O}(t_0)$ is the zero-spatial-momentum operator

$$\tilde{O}(t_0)=\sum_{\vec{x}}O(t_0,\vec{x}) \tag{2.11}$$

and $O(t\vec{x})$ is a (not necessarily local) operator function of the $U_{n\mu}$ fields, which is summed over a fixed "time slice" t_0. The parameter δ is chosen to be small, and the system E_1 is then allowed to evolve in time with the *same* noise distribution $\{\omega_{n\mu}^{\alpha}\}$ as system E_0. Note that because of the logical statements present in a Metropolis Monte Carlo procedure, phase coherence and ensuing cancellation of errors cannot be achieved for long runs. If the same operator $\tilde{O}(t)$ is then averaged over a different time slice t_1, one has for system E_0

$$\langle\tilde{O}(t_1)\rangle_{E_0}=\frac{\int[dU]\tilde{O}(t_1)e^{-S[U]}}{\int[dU]e^{-S[U]}} \tag{2.12}$$

while for system E_1 one obtains

$$\langle \tilde{O}(t_1)\rangle_{E_1}=\frac{\int [dU]\tilde{O}(t_1)e^{-S[U]+\delta\tilde{O}(t_0)}}{\int [dU]e^{-S[U]+\delta\tilde{O}(t_0)}}$$

$$=\langle \tilde{O}(t_1)\rangle_{E_0}+\delta\frac{\int [dU]\tilde{O}(t_1)\tilde{O}(t_0)e^{-S[U]}}{\int [dU]e^{-S[U]}}-\delta\frac{\int [dU]\tilde{O}(t_1)e^{-S[U]}\int [dU]\tilde{O}(t_0)e^{-S[U]}}{\left[\int [dU]e^{-S[U]}\right]^2}+O(\delta^2)\,. \tag{2.13}$$

From this one realizes that the connected correlation function of the operators $\tilde{O}(t)$ at distances $|t_1-t_0|$ is given by

$$\langle \tilde{O}(t_1)\tilde{O}(t_0)\rangle_c=\delta^{-1}[\langle \tilde{O}(t_1)\rangle_{E_1}-\langle \tilde{O}(t_1)\rangle_{E_0}]+O(\delta)\,. \tag{2.14}$$

For convenience we have chosen the measured operator $[\tilde{O}(t_1)]$ and the one in the action $[\tilde{O}(t_0)]$ to be the same, but the method of course allows for the possibility of having different operators $\tilde{O}_\alpha(t_1)$ and $\tilde{O}_\beta(t_0)$ on different times slices, and study their mixing. In this framework one can also gain information about the mixing between glueballs and operators containing fermion fields. One considers, for example, a glueball operator $\tilde{O}(t_0)$ added to the action and measures on the remaining time slices the expectation value of the meson operator

$$\sum_{\vec{x}}\bar{\psi}(\vec{x},t)\Gamma\psi(\vec{x},t)\,, \tag{2.15}$$

where Γ is a Dirac gamma matrix. After formal integration over the Fermi fields the above operator is replaced by the matrix element of the inverse of the lattice Dirac operator

$$\sum_{\vec{x}}\mathrm{Tr}\left\langle \vec{x},t\left|\frac{\Gamma}{\not{D}+m}\right|\vec{x},t\right\rangle \tag{2.16}$$

evaluated in a background gauge configuration.

In the present study we limited ourselves to the one-plaquette operator summed over spatial orientations

$$\tilde{O}(t)=\tfrac{1}{6}\sum_{\vec{x}}\mathrm{Tr}[U_P(\vec{x},t)+\mathrm{H.c.}]\,. \tag{2.17}$$

The change in the action induced on one time slice amounts in this case to an increase in the inverse gauge coupling $\beta\to\beta+\delta$ on the same slice. The operator in (2.17) has the correct spin-parity assignment for the $J^{PC}=0^{++}$ glueball state.

III. NUMERICAL RESULTS

In this section we present the results of a numerical simulation using the discretized Langevin equation (2.7). First we want to show that this provides an alternative way to create equilibrium configurations of the SU(3) lattice gauge theory. To this end we did runs on a $4\times4\times4\times4$ lattice from ordered starts at $\beta=5.6$ with $\epsilon=0.001$ and 0.0025. Figure 1 shows a graph of the average action per plaquette as a function of the number of sweeps through the lattice. As one can see it converges to the right value known from Monte Carlo simulations. The magnitude of ϵ is chosen as a compromise between two requirements: it has to be small since every step introduces an error of order ϵ. It should not be too small, because smaller ϵ provides slower convergence to equilibrium (see Fig. 1). We have found that $\epsilon=0.001$ to 0.0025 works reasonably well.

The update of a single link with the Langevin method takes about twice as long as in conventional Monte Carlo algorithms. The main reason for this is the need to project out the anti-Hermitian traceless part of $(\partial S/\partial U_{n\mu})U_{n\mu}$ in Eq. (2.7). However, the advantage of the Langevin formalism is that one can measure connected correlation functions accurately as described in the previous section. We have done this for various couplings: $\beta=5.4$, 5.5, 5.6, 5.7, and 5.8. These values of β were chosen because the crossover from strong to weak-

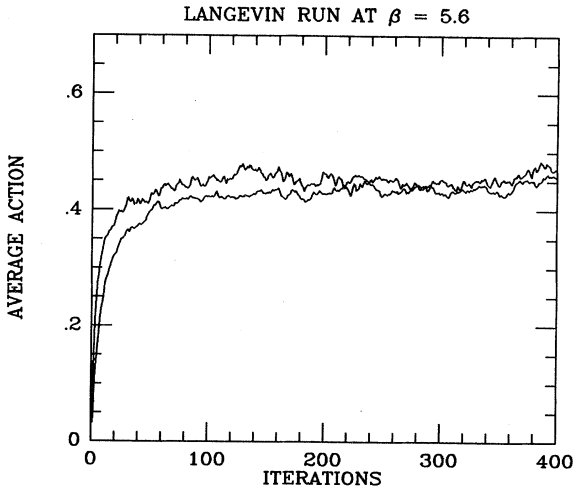

FIG. 1. Comparison of two Langevin runs at $\beta=5.6$ for $\epsilon=0.001$ (lower curve) and $\epsilon=0.0025$ (upper curve).

coupling behavior in the string tension is observed at $\beta=5.3$—5.4, which roughly coincides with the observed peak in the specific heat, and since the string tension scales according to the asymptotic-freedom formula for $\beta=5.4$—6.0. The lattice used should be big enough to accurately represent long-wavelength fluctuations, which means that it should at least be somewhat larger than the correlation length. We always worked on a $6\times6\times6\times6$ symmetric lattice. Monte Carlo data for the string tension show that such a lattice should be large enough for the values of β considered here.

As explained in Sec. II, at each β we had to perform two highly correlated runs (E_0 and E_1). We started them from configurations which were previously brought to equilibrium. At $\beta=5.6$ we used a configuration which we had on tape. It was thermalized from an ordered start by 2400 Monte Carlo iterations. The starting configurations for the other couplings were obtained from this by another 500 Monte Carlo sweeps. In the Langevin runs for computing the correlation functions we used both $\epsilon=0.001$ and 0.0025 for $\beta=5.5$, 5.6, and 5.7, while at $\beta=5.4$ and 5.8 we limited ourselves to $\epsilon=0.001$. We had to stop our runs after ~400 iterations, because at that point the phase coherence between the two correlated systems was lost due to the accumulated roundoff errors. At $\beta=5.7$ we also did a run in which we set ϵ to 0.0025 for the first 100 iterations (in both systems E_0 and E_1) to speed up the approach to equilibrium, and then changed it to 0.001 to reduce the statistical fluctuations. We used $\delta=\delta\beta=0.05$ in system E_1 throughout. In all cases we were able to reproduce the correct average action per plaquette (see Table I). Figure 2 shows a plot of the average action per plaquette for the two correlated Langevin runs at $\beta=5.6$ and for $\epsilon=0.0025$. It clearly shows that the two systems E_0 and E_1 fluctuate together.

Because of our use of periodic boundary conditions we were allowed to average over forward and backward correlations. We computed

TABLE I. Comparison of the average action per plaquette. For the Langevin runs the average is over all 400 iterations of system E_0, while for the Monte Carlo runs the average is over the last 400 iterations at each β.

β	ϵ	Langevin	Monte Carlo
5.4	0.001	0.5231±0.0035	0.5239±0.0030
5.5	0.001	0.5006±0.0058	0.5017±0.0041
	0.0025	0.5009±0.0054	
5.6	0.001	0.4690±0.0095	0.4761±0.0011
	0.0025	0.4687±0.0065	
5.7	0.001	0.4442±0.0042	
	0.0025	0.4488±0.0041	0.4477±0.0021
	0.0025/1	0.4456±0.0034	
5.8	0.001	0.4278±0.0024	0.4347±0.0033

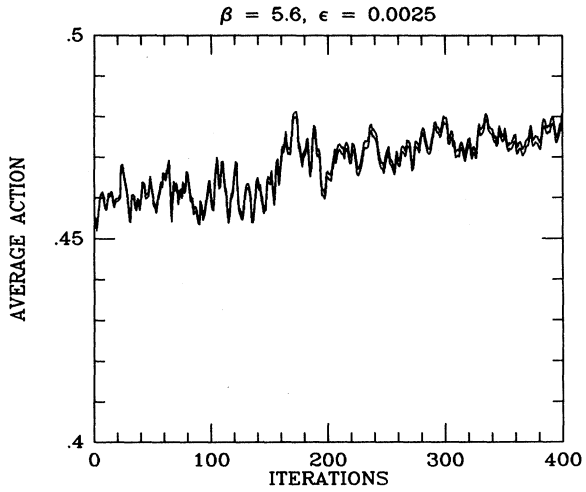

FIG. 2. Average action at $\beta=5.6$ for $\epsilon=0.0025$. In the run corresponding to the lower curve the temperature β has been raised on one time slice by an amount $\delta\beta=0.05$.

$$G(t)=\tfrac{1}{2}[\langle\tilde{O}(t_0+t)\tilde{O}(t_0)\rangle_c+\langle\tilde{O}(t_0-t)\tilde{O}(t_0)\rangle_c] \quad (3.1)$$

with $t\leq L/2$ and L the linear size of the lattice in the time direction. In Fig. 3 we show the correlation functions $G(t)$ for $t=0$, 1, 2, and 3 at $\beta=5.6$ and for $\epsilon=0.0025$. As expected, the noise in the correlation functions increases with distance. While the result for the average plaquette is not noticeably dependent on ϵ in the range we investigated, the approach to equilibrium for correlations at longer distances is considerably slower for smaller ϵ (0.001 as compared to 0.0025). This phenomenon becomes more acute when the mass gap m_G gets smaller. For large (Langevin) times we expect the relaxation time τ that governs the approach to equilibrium to scale as

$$\tau\sim m_G{}^{-z}, \quad (3.2)$$

where z is a dynamical critical exponent.[11] No estimate for this exponent is known to us for gauge theories in four dimensions. For a simple φ^4 theory near four dimensions one finds $z=2$ whereas for the O(3) Heisenberg model near $d=6$ one gets $z=4$. The rather large dynamical critical exponent for the O(3) model is connected to the presence of the global continuous symmetry and Goldstone modes.

We would expect the index z to be rather large for gauge theories as well since motions along gauge orbits cost no energy and do not drive the system toward equilibrium. In principle this difficulty could be overcome by doing longer runs. However, we had to limit our runs to 400 iterations, because after that the phase coherence between the two correlated runs was lost. Some of those problems could probably be avoided by using double precision or a 64-bit machine (we worked on a 32-bit machine). We found a somewhat improved convergence

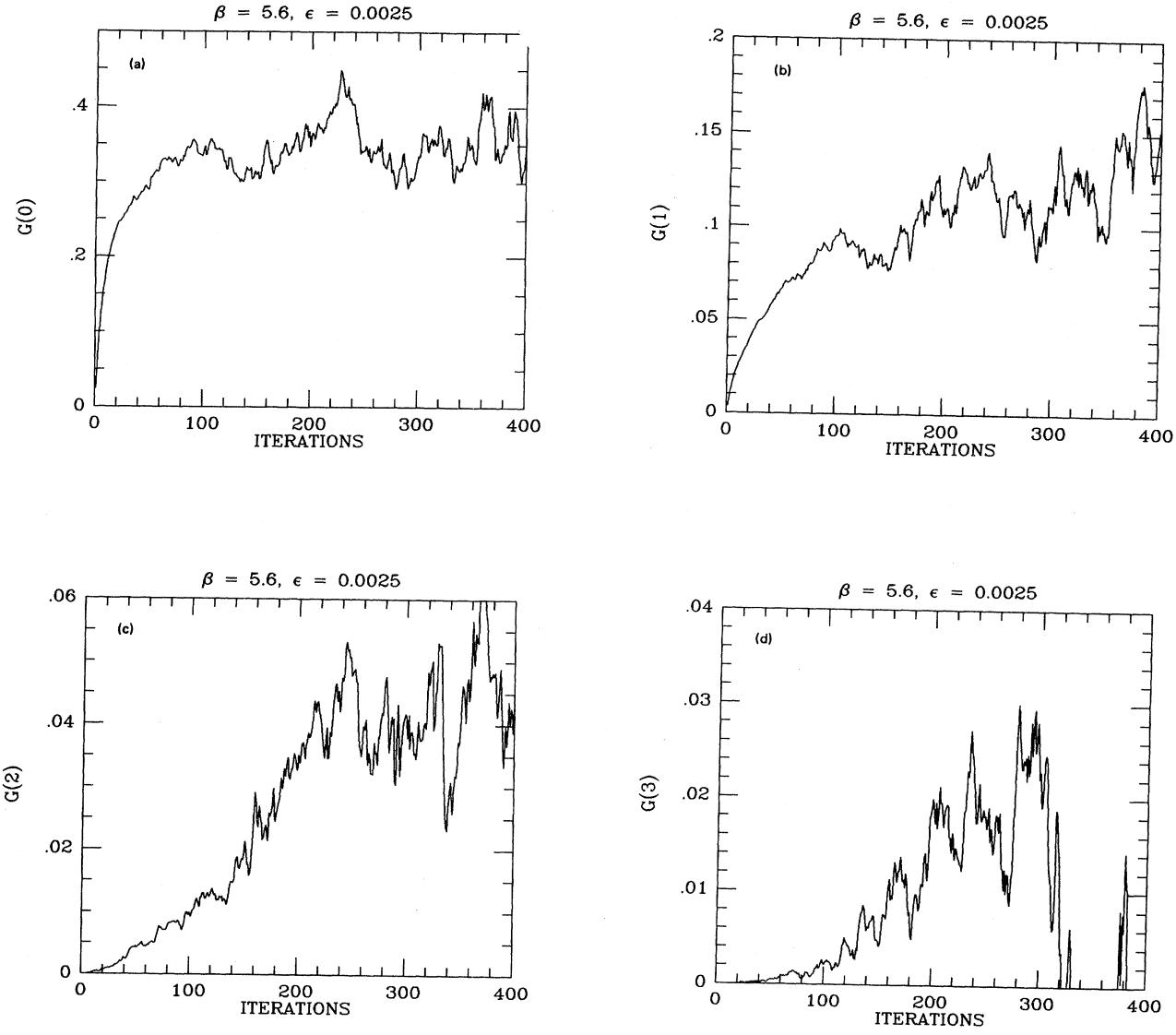

FIG. 3. Glueball correlation function for $\beta=5.6$ and $\epsilon=0.0025$ at separation 0 (a), separation 1 (b), separation 2 (c), and separation 3 (d).

rate when a bigger value of ϵ was taken at the beginning of a run and later was reduced in order to improve on the errors. The study of an optimal choice of ϵ's is beyond the scope of the present investigation.

Since the operator $\tilde{O}(t)$ we used in Eq. (3.1) is summed over all sites of the time slice t it projects out the zero-spatial-momentum part of the correlation function. When r labels the physical states that couple $\tilde{O}$ we assume that $G(t)$ behaves as

$$G(t)=\sum_r A_r \cosh\left[m_r\left[\frac{L}{2}t\right]\right]. \tag{3.3}$$

(Periodic boundary conditions have been used.) At large separations in the time direction the state with the lowest mass dominates the correlation function (3.3). For the operator used [Eq. (2.17)] this is presumably the $J^{PC}=0^{++}$ glueball. We were not able to measure $G(t)$ for long enough times to make a fit of the form (3.3). Instead we used a one-mass parametrization of $G(t)$ and extracted a distance-dependent mass $m(t)$ from

$$\frac{G(t)}{G(t-1)}\equiv\frac{\cosh[m(t)(L/2-t)]}{\cosh\{m(t)[L/2-(t-1)]\}}. \tag{3.4}$$

The lowest mass m_0 is then found as

TABLE II. Correlation functions $G(t)$ $(t=0,\ldots,3)$ for various values of β and ϵ, averaged over clusters of 50 iterations with standard deviation in each cluster.

	Cluster number	Correlation functions $t=0$	$t=1$	$t=2$	$t=3$
$\beta=5.4$	1	0.1581±0.0086	0.0233±0.0015	0.0002±0.0000	0.0000±0.0000
$\epsilon=0.001$	2	0.2687±0.0030	0.0484±0.0008	0.0010±0.0000	0.0000±0.0000
	3	0.3250±0.0017	0.0662±0.0006	0.0017±0.0000	0.0000±0.0000
	4	0.3705±0.0015	0.0812±0.0010	0.0033±0.0002	0.0003±0.0001
	5	0.3815±0.0013	0.0901±0.0007	0.0029±0.0002	0.0009±0.0000
	6	0.3646±0.0017	0.1011±0.0008	0.0013±0.0004	−0.0018±0.0001
	7	0.4414±0.0037	0.1126±0.0008	0.0055±0.0004	0.0015±0.0004
	8	0.4634±0.0030	0.1254±0.0023	0.0235±0.0015	0.0095±0.0004
$\beta=5.5$	1	0.1617±0.0087	0.0236±0.0015	0.0002±0.0000	0.0000±0.0000
$\epsilon=0.001$	2	0.2622±0.0018	0.0501±0.0007	0.0012±0.0000	0.0001±0.0000
	3	0.3241±0.0026	0.0713±0.0009	0.0024±0.0001	0.0003±0.0000
	4	0.3620±0.0022	0.0914±0.0009	0.0033±0.0001	0.0007±0.0000
	5	0.4034±0.0036	0.0942±0.0005	0.0043±0.0002	0.0020±0.0001
	6	0.4364±0.0016	0.1009±0.0008	0.0046±0.0003	0.0048±0.0002
	7	0.4175±0.0021	0.0985±0.0014	−0.0002±0.0006	0.0013±0.0003
	8	0.3811±0.0043	0.1087±0.0024	−0.0017±0.0011	−0.0078±0.0004
$\beta=5.5$	1	0.2416±0.0108	0.0433±0.0025	0.0013±0.0001	0.0000±0.0000
$\epsilon=0.0025$	2	0.3607±0.0037	0.0857±0.0014	0.0048±0.0002	0.0010±0.0001
	3	0.3909±0.0020	0.1047±0.0014	0.0085±0.0004	0.0043±0.0003
	4	0.3754±0.0033	0.1082±0.0032	0.0039±0.0011	0.0068±0.0005
	5	0.3599±0.0078	0.0939±0.0079	−0.0085±0.0021	−0.0012±0.0016
	6	0.5601±0.0133	0.2054±0.0096	−0.0206±0.0040	−0.0705±0.0060
	7	0.3534±0.0266	0.2401±0.0203	−0.0604±0.0092	−0.1001±0.0102
	8	0.2684±0.0467	0.7452±0.0276	0.2585±0.0392	0.1304±0.0298
$\beta=5.6$	1	0.1714±0.0089	0.0254±0.0016	0.0003±0.0000	0.0000±0.0000
$\epsilon=0.001$	2	0.2665±0.0017	0.0508±0.0008	0.0016±0.0001	0.0001±0.0000
	3	0.3023±0.0010	0.0666±0.0007	0.0040±0.0002	0.0003±0.0000
	4	0.3376±0.0024	0.0809±0.0008	0.0068±0.0001	0.0008±0.0000
	5	0.3622±0.0007	0.0914±0.0003	0.0077±0.0002	0.0004±0.0000
	6	0.3978±0.0031	0.1090±0.0009	0.0141±0.0003	0.0008±0.0001
	7	0.4332±0.0022	0.1239±0.0006	0.0160±0.0002	−0.0012±0.0001
	8	0.4418±0.0013	0.1273±0.0008	0.0214±0.0008	0.0042±0.0004
$\beta=5.6$	1	0.2306±0.0094	0.0421±0.0024	0.0014±0.0002	0.0001±0.0000
$\epsilon=0.0025$	2	0.3312±0.0018	0.0802±0.0012	0.0068±0.0003	0.0011±0.0001
	3	0.3249±0.0025	0.0863±0.0009	0.0134±0.0004	0.0043±0.0003
	4	0.3417±0.0026	0.1039±0.0017	0.0269±0.0008	0.0105±0.0005
	5	0.3887±0.0040	0.1221±0.0013	0.0419±0.0008	0.0182±0.0005
	6	0.3238±0.0024	0.1053±0.0014	0.0389±0.0007	0.0197±0.0009
	7	0.3435±0.0026	0.1187±0.0018	0.0384±0.0011	0.0030±0.0016
	8	0.3624±0.0047	0.1438±0.0025	0.0479±0.0011	−0.0132±0.0016
$\beta=5.7$	1	0.1628±0.0083	0.0245±0.0015	0.0004±0.0000	0.0000±0.0000
$\epsilon=0.001$	2	0.2582±0.0021	0.0471±0.0007	0.0019±0.0001	0.0002±0.0000
	3	0.2835±0.0013	0.0598±0.0004	0.0035±0.0001	0.0006±0.0000
	4	0.3012±0.0004	0.0669±0.0003	0.0042±0.0001	0.0008±0.0000
	5	0.3016±0.0005	0.0710±0.0002	0.0054±0.0001	0.0011±0.0000
	6	0.3001±0.0016	0.0776±0.0004	0.0075±0.0002	0.0010±0.0001
	7	0.3271±0.0011	0.0790±0.0007	0.0101±0.0001	0.0003±0.0001
	8	0.3326±0.0011	0.0822±0.0005	0.0097±0.0002	−0.0002±0.0001

TABLE II. (*Continued.*)

	Cluster number	Correlation functions $t=0$	$t=1$	$t=2$	$t=3$
$\beta=5.7$	1	0.2269±0.0089	0.0417±0.0023	0.0018±0.0002	0.0001±0.0000
$\epsilon=0.0025$	2	0.3140±0.0024	0.0738±0.0009	0.0051±0.0001	0.0012±0.0001
	3	0.3305±0.0017	0.0829±0.0006	0.0082±0.0003	0.0002±0.0001
	4	0.3289±0.0017	0.0897±0.0010	0.0120±0.0004	−0.0001±0.0003
	5	0.3413±0.0022	0.0809±0.0018	0.0089±0.0011	0.0017±0.0007
	6	0.3165±0.0032	0.0845±0.0018	0.0250±0.0018	0.0115±0.0014
	7	0.4644±0.0140	0.1282±0.0083	0.0060±0.0025	0.0229±0.0039
	8	0.5082±0.0075	0.1932±0.0056	−0.0338±0.0034	−0.0347±0.0040
$\beta=5.7$	1	0.2269±0.0089	0.0417±0.0023	0.0018±0.0002	0.0001±0.0000
$\epsilon=0.0025$	2	0.3140±0.0024	0.0738±0.0009	0.0051±0.0001	0.0012±0.0001
−0.001	3	0.3366±0.0010	0.0869±0.0004	0.0077±0.0002	0.0010±0.0001
	4	0.3431±0.0009	0.0836±0.0004	0.0080±0.0001	−0.0007±0.0001
	5	0.3294±0.0013	0.0887±0.0005	0.0080±0.0001	0.0036±0.0003
	6	0.2993±0.0018	0.0855±0.0007	0.0174±0.0007	0.0079±0.0003
	7	0.3345±0.0016	0.0998±0.0007	0.0188±0.0004	0.0082±0.0005
	8	0.3411±0.0031	0.1103±0.0008	0.0206±0.0010	0.0011±0.0005
$\beta=5.8$	1	0.1581±0.0080	0.0242±0.0015	0.0004±0.0000	0.0000±0.0000
$\epsilon=0.001$	2	0.2486±0.0017	0.0473±0.0006	0.0015±0.0000	0.0000±0.0000
	3	0.2685±0.0008	0.0551±0.0003	0.0035±0.0001	0.0004±0.0000
	4	0.2794±0.0007	0.0627±0.0005	0.0054±0.0001	0.0005±0.0000
	5	0.2892±0.0014	0.0660±0.0003	0.0065±0.0000	0.0010±0.0000
	6	0.2878±0.0007	0.0697±0.0004	0.0071±0.0001	0.0018±0.0001
	7	0.2994±0.0009	0.0767±0.0003	0.0090±0.0001	0.0023±0.0001
	8	0.3010±0.0013	0.0774±0.0005	0.0079±0.0001	0.0008±0.0002

$$\lim_{\substack{t\to\infty \\ L\gg t}} m(t)=m_0 \ . \tag{3.5}$$

We assume that the gap between m_0 and higher masses that contribute to $G(t)$ in (3.3) is large enough that $m(t)$ gives a good estimate for m_0 already at small distances.

In order to extract the correlation functions and mass estimates we chose to average the correlation functions over 8 clusters of 50 iterations. The result, including the standard deviation in each cluster, is presented in Table II. Since the equilibrium values of the correlation functions and mass estimates are reached at large Langevin time (number of iterations), we have to extrapolate our results. We can proceed in two different ways.

(i) Extrapolation of the correlation functions. We fit the cluster averages of Table II as a function of $1/N$ where N is the number of the cluster, and extrapolate to $1/N=0$. For this we made a polynomial fit

$$G\left[t,\frac{1}{N}\right]=G(t,0)+\alpha(t)\frac{1}{N}+b(t)\frac{1}{N^2} \ . \tag{3.6}$$

TABLE III. Mass estimates for various value of β and ϵ. The mass values are the average of the two extrapolation procedures (see text) and the error estimates their differences.

β	ϵ	$m(1)$	$m(2)$	$m(3)$
5.4	0.001	1.16±0.06	2.2±0.9	1.7±1.0
5.5	0.001	1.26±0.05	2.8±0.2	1.3±0.4
	0.0025	0.95±0.10	2.7±0.8	1.3±0.9
5.6	0.001	1.11±0.05	1.4±0.4	2.7±0.6
	0.0025	0.91±0.05	0.8±0.3	1.0±0.2
5.7	0.001	1.25±0.05	1.9±0.2	2.3±0.5
	0.0025	1.20±0.15	1.6±0.6	1.3±0.5
	0.0025/1	1.12±0.05	1.45±0.2	1.4±0.5
5.8	0.001	1.26±0.05	1.75±0.3	1.6±0.3

The masses $m(t)$ are then extracted from $G(t,0)$ as in Eq. (3.4).

(ii) Extrapolation of the mass estimates. For each cluster calculate the masses $m(t,1/N)$ from (3.4), fit them as a function of $1/N$, and extrapolate to $1/N=0$. Again we used a polynomial fit similar to Eq. (3.6).

The two methods provide us with two estimates for the distance-dependent masses. In Table III we list the average of the two for the various values of β and ϵ. The error induced by the extrapolation procedure can be estimated as the difference between the two values for the masses obtained in (i) and (ii). It is also quoted in Table III.

At longer distances the mass estimates from the runs with $\epsilon=0.001$ tend to be larger than the ones from runs with $\epsilon=0.0025$. This is probably due to the fact that relaxation for $\epsilon=0.001$ takes much longer and has not been achieved in those runs. In all cases we have observed that, not unexpectedly, the approach to equilibrium for the correlation functions (and hence the masses) at longer distances is much slower. The mass estimates at distances 2 and 3 come therefore with larger errors than at distance 1. In Fig. 4 we show these mass estimates as a function of β. At $\beta=5.4$ and 5.8, $\epsilon=0.001$ was used, whereas at the other β's the results from the runs with $\epsilon=0.0025$ are plotted. Also shown in Fig. 4 are the spin-wave estimates for weak coupling (for $t=2$ and 3) and the scaling curves predicted from asymptotic freedom.

IV. DISCUSSION

Let us now come to a discussion of our results. In order to extrapolate the glueball mass to the continuum limit ($\beta=\infty$) we use the renormalization group. Define the lattice scale parameter for SU(3):

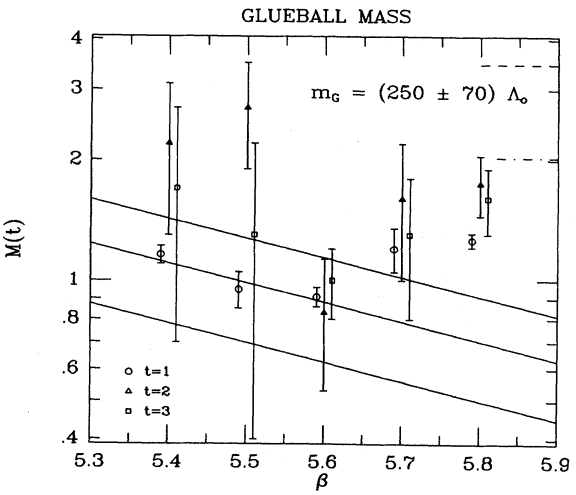

FIG. 4. 0^{++}-glueball-mass estimates at different couplings for different separations. The continuous lines represent the expected renormalization-group behavior $m_G=(240\pm70)\Lambda_0$. The dashed and dashed-dotted lines represent the expected weak-coupling spin-wave behavior of the distance-dependent masses [Eq. (3.4)] $m(1)$ and $m(2)$.

$$\Lambda_0=\alpha^{-1}\left[\frac{8\pi^2}{33}\beta\right]^{51/121} e^{-(4\pi^2/33)\beta}[1+O(\beta^{-1})]\,. \tag{4.1}$$

Then for large β we expect the glueball mass to scale as

$$m_G=c\Lambda_0\,. \tag{4.2}$$

It is not clear from our data to what extent the values for m_G seem to follow this prediction. The mass estimates at $\beta=5.4$, 5.5, and 5.6 are consistent with the expected behavior, although the values at larger separation have large error bars due to the statistical fluctuations. (For larger mass the correlation functions decrease more rapidly and are therefore more difficult to measure.)

The situation, however, is not so nice if one considers what happens to the specific heat in the same region. By the Monte Carlo method we have computed the energy density between $\beta=4.5$ and 6.5 using an increment $\delta\beta=0.03$ and 80 iterations for each value of β on a $5\times5\times5\times5$ lattice, averaging over the last 40 iterations. An eight-order polynomial fit to this data was then performed, and from it the derivative was estimated. From this analysis we find a peak in the specific heat at $\beta=5.5$–5.6, which can probably be ascribed to a nearby complex zero of the partition function. If a singularity were to appear for a real $\beta=\beta_c$, then a scaling argument would suggest

$$\frac{\partial E}{\partial\beta}\underset{\beta\to\beta_c}{\sim} A\,|\beta-\beta_c|^{-\alpha} \sim Bm^{(d\nu-2)/\nu}\,, \tag{4.3}$$

where α and ν are critical exponents, m is the inverse of the correlation length, and A and B are regular functions for $\beta\to\beta_c$. This would in turn imply that m goes to zero as

$$m\underset{\beta\to\beta_c}{\sim}\left|B^{-1}\frac{\partial E}{\partial\beta}\right|^{\nu/(d\nu-2)}\,. \tag{4.4}$$

In the case of SU(3) lattice gauge theories with the Wilson action it seems unlikely that the peak in the specific heat will not have some effect on the glueball mass (a dip) around and before $\beta=5.6$, a behavior that is unrelated to the asymptotic freedom scaling expected for large β. A similar behavior is also observed in the string tension and the hadron masses. Therefore we conclude that our estimates for $\beta<5.6$ are likely to be affected by at present uncontrollable systematic effects due to nearby spurious singularities.

On the other hand, at large β ($\beta\gtrsim5.7$) we see that our data clearly deviates from the asymptotic-freedom prediction. Indeed it is known that for weak enough coupling the spin-wave result

$$G(t)\sim t^{-5} \tag{4.5}$$

should be recovered for small enough distances, $t\ll m_G{}^{-1}$. In Fig. 4 we have included the spin-wave pre-

diction for the distance-dependent mass estimates $m(2)$ and $m(3)$ defined in the preceding section. Since we are limited, because of the size of our $6\times6\times6\times6$ lattice, to separations of up to three lattice spacings, we are at the present unable to penetrate more deeply into the scaling region. It would seem therefore that our most believable point, as far as the extrapolation to $\beta\to\infty$ is concerned, is $\beta=5.6$. Our conclusion is thus

$$m_G=(240\pm70)\Lambda_0\ . \tag{4.6}$$

An alternative way of presenting our results would be as a ratio of the 0^{++} glueball mass to a known physical quantity also accessible by the Monte Carlo method. Using recent high-statistics data for the string tension on an $8\times8\times8\times8$ lattice[20] we find at $\beta=5.6$

$$\frac{m_G}{\sqrt{T}}=\frac{(0.9\pm0.1)\alpha^{-1}}{(0.35\pm0.05)\alpha^{-1}}=2.6\pm1.0\ . \tag{4.7}$$

The string tension is not known directly, but if we use $T=(420\text{ MeV})^2$ we get $m_G=1080\pm400$ MeV.

In Ref. 16 the ρ mass at $\beta=5.6$ was estimated to be $m_\rho=(0.8\pm0.1)\alpha^{-1}$ using the Wilson fermion action[10] on a lattice of maximum size $6\times6\times6\times12$. From this estimate we obtain

$$\frac{m_G}{m_\rho}=\frac{(0.9\pm0.1)\alpha^{-1}}{(0.8\pm0.1)\alpha^{-1}}=1.1\pm0.2 \tag{4.8}$$

which would give, using the physical ρ mass as input, for the mass of the lowest glueball about 850 ± 200 MeV.

Let us finally briefly compare our results with previous estimates. Our values for the masses at different coupling constants are in reasonable agreement with previous results, although they usually tend to be slightly lower. In the first of Ref. 15 the finite-size scaling method was used to estimate the mass of the scalar glueball at $\beta=6.0$, giving the large value $(1.2\pm0.1)\alpha^{-1}$ at separations 2 and 3 on lattices of maximum size $7\times7\times7\times7$, an estimate that now would seem to be contaminated by the spin-wave behavior of Eq. (4.5). The variational estimate of Ref. 6 at $\beta=5.7$ on a $4\times4\times4\times8$ lattice is about 30% above our best result in terms of Λ_0. However, at the coupling our masses seem already to be influenced by the spin-wave behavior as well. The same technique was used to estimate the glueball mass in Ref. 7 at several values of β ranging from 5.0 to 5.8 on a $4\times4\times4\times8$ lattice. Their latest estimate is about 15% higher than ours, but the agreement seems good in view of the different techniques used.

Several explanations for the discrepancies are possible. Among these we mention the slightly larger lattice used in the present calculation and the influence of the peak in the specific heat, which might be size dependent. It now seems important that longer runs on larger lattices be done. Work in this direction is in progress and will be reported elsewhere.

ACKNOWLEDGMENTS

One of us (H.H.) would like to thank E. Marinari and G. Parisi for many fruitful discussions on the Langevin equation. We have written together part of the code that was later adapted for the present study. This research was supported by the U.S. Department of Energy under Grant No. DE-AC02-76ER02220. U.H. wishes to express his thanks for a grant by the Federal Republic of Germany.

[1]J. Kogut, D. K. Sinclair, and L. Susskind, Nucl. Phys. B114, 199 (1976).

[2]C. Rebbi, in *Proceedings of the 21st International Conference on High Energy Physics, Paris, 1982,* edited by P. Petiau and M. Porneuf [J. Phys. (Paris) Colloq. 43, (1982)].

[3]G. Bhanot and C. Rebbi, Nucl. Phys. B180 [FS2], 469 (1981).

[4]B. Berg, in *Lattice Gauge Theories, Supersymmetry, and Grand Unification,* proceedings of the 6th Johns Hopkins Workshop on Current Problems in Particle Theory, Florence, 1982 (Physics Department, Johns Hopkins University, Baltimore, 1982).

[5]M. Falcioni *et al.*, Phys. Lett. 110B, 295 (1982).

[6]K. Ishikawa, G. Schierholz and M. Teper, Phys. Lett. 110B, 399 (1982); 116B, 429 (1982); 120B, 387 (1983); DESY Report No. 83-04 (unpublished).

[7]B. Berg and A. Billoire, Phys. Lett. 113B, 65 (1982); 114B, 324 (1982); Nucl. Phys. B221, 109 (1983).

[8]K. H. Mütter and K. Schilling, Phys. Lett. 117B, 75 (1982); 121B, 267 (1983).

[9]M. Falcioni *et al.*, Nucl. Phys. B215 [FS7], 265 (1983).

[10]K. G. Wilson, Phys. Rev. D 10, 2445 (1974); in *New Phenomena in Subnuclear Physics,* Proceedings of the 14th Course of the International School of Subnuclear Physics, Erice, 1975, edited by A. Zichichi (Plenum, New York, 1976).

[11]B. Halperin and P. C. Hohenberg, Rev. Mod. Phys. 49, 435 (1977).

[12]G. Parisi and Wu Yong-Shi, Sci. Sin. 24, 483 (1980).

[13]G. Parisi, Nucl. Phys. B180 [FS2], 378 (1981); B205 [FS5], 337 (1982).

[14]I. Drummond, S. Duane, and R. Horgan, Cambridge University Report No. DAMPT 82/19, 1982 (unpublished).

[15]H. Hamber and G. Parisi, Phys. Rev. Lett. 47, 1795 (1981); E. Marinari, G. Parisi, and C. Rebbi, *ibid.* 47, 1798 (1981).

[16]H. Hamber and G. Parisi, Phys. Rev. D 27, 208 (1983).

[17]G. Parisi (unpublished).

[18]J. Alfaro and B. Sakita, CCNY Report No. HEP-82/16, 1982 (unpublished); A. Guha and S. C. Lee, Phys. Rev. D 27, 2412 (1983).

[19]We thank E. Marinari for suggestions on this point.

[20]M. Creutz, R. Ardill, and K. Moriarty, Brookhaven Report No. BNL-32377, 1982 (unpublished).